

Past and future of trypanosomatids high-throughput phenotypic screening

Rafael Ferreira Dantas¹, Eduardo Caio Torres dos Santos², Floriano Paes Silva Junior^{1/+}

¹Fundação Oswaldo Cruz-Fiocruz, Instituto Oswaldo Cruz, Laboratório de Bioquímica Experimental de Computacional de Fármacos, Rio de Janeiro, RJ, Brasil

²Fundação Oswaldo Cruz-Fiocruz, Instituto Oswaldo Cruz, Laboratório de Bioquímica de Tripanosomatídeos, Rio de Janeiro, RJ, Brasil

Diseases caused by trypanosomatid parasites affect millions of people mainly living in developing countries. Novel drugs are highly needed since there are no vaccines and available treatment has several limitations, such as resistance, low efficacy, and high toxicity. The drug discovery process is often analogous to finding a needle in the haystack. In the last decades a so-called rational drug design paradigm, heavily dependent on computational approaches, has promised to deliver new drugs in a more cost-effective way. Paradoxically however, the mainstay of these computational methods is data-driven, meaning they need activity data for new compounds to be generated and available in databases. Therefore, high-throughput screening (HTS) of compounds still is a much-needed exercise in drug discovery to fuel other rational approaches. In trypanosomatids, due to the scarcity of validated molecular targets and biological complexity of these parasites, phenotypic screening has become an essential tool for the discovery of new bioactive compounds. In this article we discuss the perspectives of phenotypic HTS for trypanosomatid drug discovery with emphasis on the role of image-based, high-content methods. We also propose an ideal cascade of assays for the identification of new drug candidates for clinical development using leishmaniasis as an example.

Key words: trypanosomatids - phenotypic - high-content screening - bioimaging - drug discovery

Trypanosomatids and neglected tropical diseases - Trypanosomatids (Euglenozoa: Kinetoplastea) are a group of protozoan obligatory parasites.^(1,2) Most members of this group are monoxenous (single host parasites) and infect invertebrates.⁽³⁾ However, some dioxenous (parasites with two intermediate hosts) species act as etiological agents of neglected tropical diseases, such as Chagas disease (*Trypanosoma cruzi*), African trypanosomiasis (*T. brucei*) and human leishmaniasis (more than 20 species).^(2,3,4) Here, we will mainly focus on the *T. cruzi* and species from the *Leishmania* genus.

Recent estimates suggest that 6 to 7 million people worldwide may be infected with *T. cruzi*, mainly in Latin America, and 75 million are at risk of infection.⁽⁵⁾ The classic route of transmission to humans is through hematophagous triatomine bugs infected with the parasite. This occurs during or right after the blood meal when the insect defecates on host skin. Its feces contain the metacyclic trypomastigote evolutionary form of *T. cruzi* which is able to penetrate the skin through the wound bite, other skin lesions or mucous membranes. Once inside the host, the parasites infect numerous types of cells, especially those from the reticuloendothelial system, muscular and nervous cells. After the infection, the parasites differentiate into amastigote forms which

proliferate by binary fission. After several replication cycles, they evolve into trypomastigotes that disrupt the cell and reach the bloodstream, allowing them to invade other cells in the organism or be taken up by another triatomine bug, continuing the parasite life cycle.⁽⁶⁾

Trypanosoma cruzi infection is responsible for the clinical outcomes of Chagas disease ranging from no apparent symptoms to severe and potentially deadly cardiovascular and/or gastrointestinal manifestations.⁽⁷⁾ This variability has been associated with factors related to both host and parasite.⁽⁸⁾ One possible explanation may be derived from parasites' genetic background. These parasites show a high genetic variability being assembled into seven distinct genetic groups, or discrete typing units (DTU): TcI-VI and TcBat.⁽⁹⁾ All of them can infect humans and their frequency varies depending on the geographic location.^(8,9) The link between *T. cruzi* genotype and the clinical manifestations (or drug susceptibility) of Chagas disease has been proposed but has not been proved yet.^(6,7,9) So far, there is no vaccine available and only two drugs, benznidazole (**1**) and nifurtimox (**2**), are clinically used. Nonetheless, they have several limitations, such as long treatment regimes, undesirable side effects (e.g., nausea, severe dermatitis and peripheral neuropathies) and clinical failure is not uncommon.⁽⁶⁾

The trypanosomatids from the *Leishmania* genus are the causal agents of one of the most devastating infectious diseases of our time: leishmaniasis.⁽¹⁰⁾ This disease affects millions of people worldwide and it is estimated that more than 1 billion are at risk of infection.⁽⁴⁾ Leishmaniasis is encountered in three main clinical forms: cutaneous (CL), visceral or kala-azar (VL) and mucocutaneous (MCL). The former is the most common while VL the most severe (fatal in more than 95 % of cases if left untreated) and MCL the most disabling.⁽¹¹⁾ Each form is elicited by a group of *Leishmania* species which include:

doi: 10.1590/0074-02760210402

Financial support: CNPq, CAPES, FAPERJ, FAPEG, FIOCRUZ.

ECTS and FPSJr are CNPq research fellows and FAPERJ CNE fellowships recipients.

+ Corresponding author: floriano@ioc.fiocruz.br

● <https://orcid.org/0000-0003-4560-1291>.

Received 20 December 2021

Accepted 28 December 2021



L. major, *L. tropica*, *L. braziliensis*, *L. amazonensis*, *L. guyanensis* for CL, *L. donovani* and *L. infantum* (also known as *L. chagasi*) for VL and *L. braziliensis*, *L. panamensis* and *L. amazonensis* for MCL.⁽¹²⁾ Regardless of the species, in most cases the parasites are transmitted to humans by the bite of infected female phlebotomine sand flies. During the blood meal, the insect's saliva and the metacyclic promastigote form of the parasite are inoculated into the host. The latter induces a phagocytic response which allows the parasite to enter the macrophage (or other mononuclear phagocytic cells) and form the parasitophorous vacuole. Inside this compartment, it differentiates into proliferating amastigote forms. Part of these infected cells can be taken up by the insect in another blood meal helping to maintain the parasite life cycle. In the human host, the continuous proliferation of amastigotes eventually leads to cell disruption and consequently release of the parasites, allowing them to infect other cells.^(13,14)

Leishmania infection is responsible for the clinical features of leishmaniasis. For VL, the most fatal form of this disease, they include persistent irregular fever, splenomegaly, pancytopenia, hepatomegaly, and hyperpigmentation of the skin (hence the name kala-azar which can be translated as "black fever"). The CL form is not life-threatening but can lead to significant cosmetic morbidity due to the scars that arise after the healing of chronic skin lesions.^(15,16) In turn, MCL is mainly characterised by the presence of ulcers in the nasal septum, lips and palate. As for VL, this form may lead to death if not treated rapidly.⁽¹⁶⁾ Currently, there is no vaccine available, and the pharmacological treatments rely on a few drugs: pentavalent antimonials [e.g., meglumine antimoniate (3)], amphotericin B (4), pentamidine (5), paromomycin (6) and miltefosine (7) (Fig. 1). In most cases, the treatment is very broad and does not take into the account the peculiarities of each species. These drugs also have some major drawbacks, such as high cost, significant toxicity, must be administered via parenteral route [except miltefosine (7)] and may induce resistance.⁽¹⁰⁾

Phenotypic-based assays in trypanosomatid drug discovery - The limitations of the current anti-trypanosomatid agents demand the search for new pharmacological alternatives. In this context, phenotypic-based assays play a pivotal role in trypanosomatid drug discovery.^(17,18,19) Most traditional methods use manual microscopy techniques (e.g., giemsa staining^(20,21,22,23)) to evaluate the effect of a given compound on the number (amastigotes) or presence/motility (promastigotes) of the parasites.^(12,24) For instance, during a typical assay using intracellular amastigote forms, a microscope operator visually counts the number of host cells (100-500 per sample⁽²⁵⁾) and intracellular parasites. From this analysis it is possible to calculate the percentage of infected cells (infection ratio), as well the average number of parasites per cell, which are used as metrics to measure compound antiparasitic activity.^(20,21,22,25,26) As expected, these methods are semi-quantitative, have low throughput and are prone to human errors. In an attempt to overcome these limitations, several phenotypic assays

have been developed using more automated technologies such as, microplate readers, flow cytometers and high-content microscopes (discussed in the next section)^(12,19,27) (Fig. 2). The most common methods rely on fluorometric, luminescence or colorimetric readouts to measure parasites viability/growth in microplate readers, which are available in many laboratories. Trypanosomatids viability has been mainly assessed by measuring parasites ATP^(28,29,30,31) content and/or by measuring the metabolic reduction of redox probes, such as tetrazolium salts (MTT/XTT/MTS)^(32,33,34) and resazurin.^(35,36,37) The number of parasites has also been indirectly obtained by SYBR Green,^(38,39) a fluorescent nuclear probe. Some assays use transgenic parasites carrying fluorescent reporter genes (e.g., GFP^(40,41,42) and mCherry⁽⁴³⁾) or reporter enzymes (e.g., beta-galactosidase,^(41,44,45,46) beta-lactamase,^(47,48) luciferase^(49,50,51,52)) whose activities can be readily detected in the presence of their substrates.

Although plate-reader-based assays represent a major advance in trypanosomatid drug discovery, they also show some important drawbacks. Firstly, they perform whole-well readouts which give no information regarding the number of host cells and parasites or their distribution.⁽⁵³⁾ Some of them are also prone to assay interference. For instance, coloured compounds may affect the readout of colorimetric assays.⁽⁵⁴⁾ Special attention should also be paid to hits coming from enzyme reporter-based assays since, theoretically, compounds may interfere with enzyme activity (or its substrate) and vice-versa, generating spurious results.^(44,53,54) Moreover, many assays were developed to test compounds against promastigotes^(12,30,32,33,55) and axenic amastigotes (i.e., amastigotes that are growth in culture media that simulate intracellular conditions)^(29,53,56) evolutionary forms. Though promastigotes are easy to handle and can be obtained in large amounts, which is desirable for HTS campaigns, they represent the vector-transmitted form of the parasite life cycle which is not directly involved in disease development.^(38,57,58) In turn, axenic amastigotes share more similarities with the intracellular forms, thus being more biologically relevant, and they have already been proved to be useful in library screening.^(29,53) Nonetheless, phenotypic assays based on both promastigotes and axenic amastigotes fail to some extent to identify active compounds (or reproduce their potency) on parasite intracellular forms and may generate false positives.^(29,59,60) In part, this is because these methods are unable to mimic the complex interaction between the parasite and the host cell.⁽²⁹⁾ Additionally, in order to exert its antiparasitic activity, a compound must overcome some obstacles before reaching its targets which include transpassing several cellular membranes and coping with pH changes.^(53,61,62)

Therefore, even lacking the throughput of plate-reader-based assays, the intracellular amastigote-based assays are still considered the gold standard for trypanosomatid drug discovery.^(27,29)

High content screening in trypanosomatid drug discovery - In the late 90's, a new generation of automated fluorescent microscopes emerged in the phenotypic

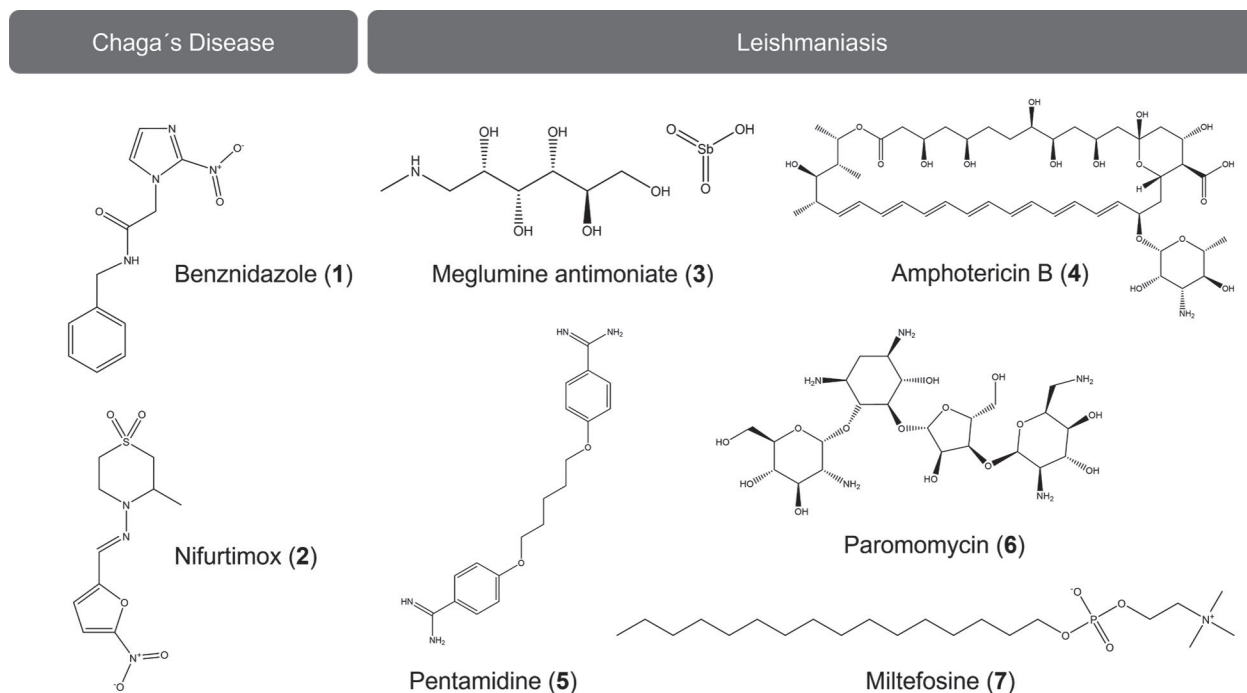


Fig. 1: clinical drugs used in the treatment of Chagas disease and leishmaniasis.

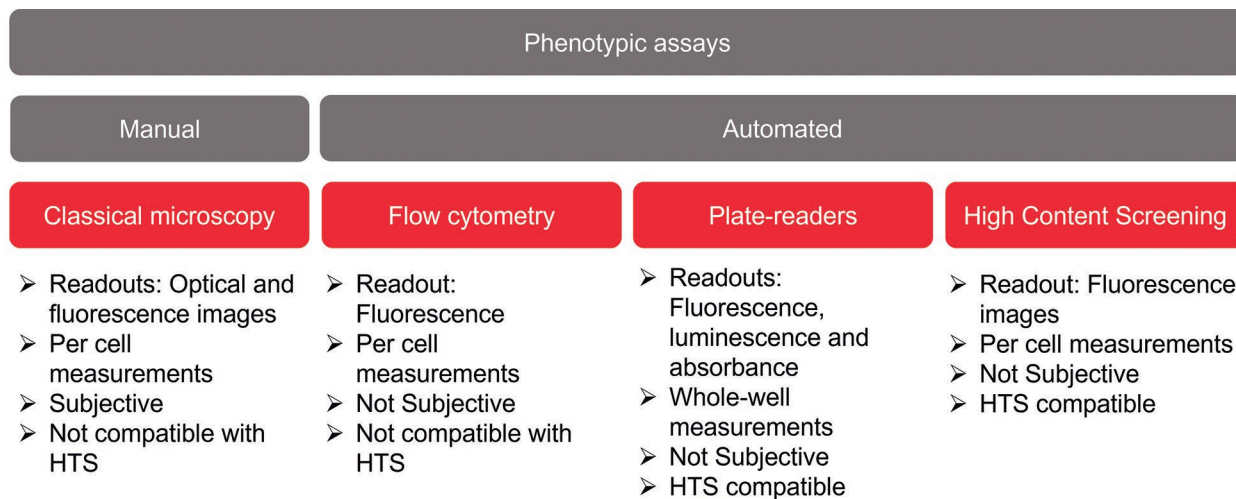


Fig. 2: main phenotypic assays used in trypanosomatid drug discovery.

drug discovery scenario.⁽⁶³⁾ This technology, also known as high-content screening (HCS), automatically extracts multiparametric data, at a single-cell level, from fluorescent microscopy images acquired in a high-throughput mode.^(63,64) HCS systems offer individual, spatial and temporal information which can be applied in different stages of the drug discovery pipeline.^(65,66) Thus, HCS-based assays have been employed in a wide range of applications.⁽⁶⁶⁾ In the context of trypanosomatid drug discovery, most reports use HCS technology to evaluate the effect of test compounds on intracellular amastigotes (Table). In these assays, host cells and parasites, distributed

in microplates, are incubated with test compounds (one or multiple concentrations for dose-response curves), stained with one^(67,68,69,70) or more^(58,71,72,73,74) fluorescent probes and their images captured in a HCS system coupled with a 10x,^(75,76) 20x (most cases^(60,73,77,78)) or 40x^(67,75) objective lens (Fig. 3A). Image analysis is performed using a custom pipeline in a proprietary (e.g., Operetta Imaging System Harmony Software, PerkinElmer^(77,79)) or free software (e.g., Cellprofiler^(58,80)). From this analysis, it is possible to obtain a few metrics used to measure compound antiparasitic activity, such as the number of amastigotes per cell and the percentage of infected cells.

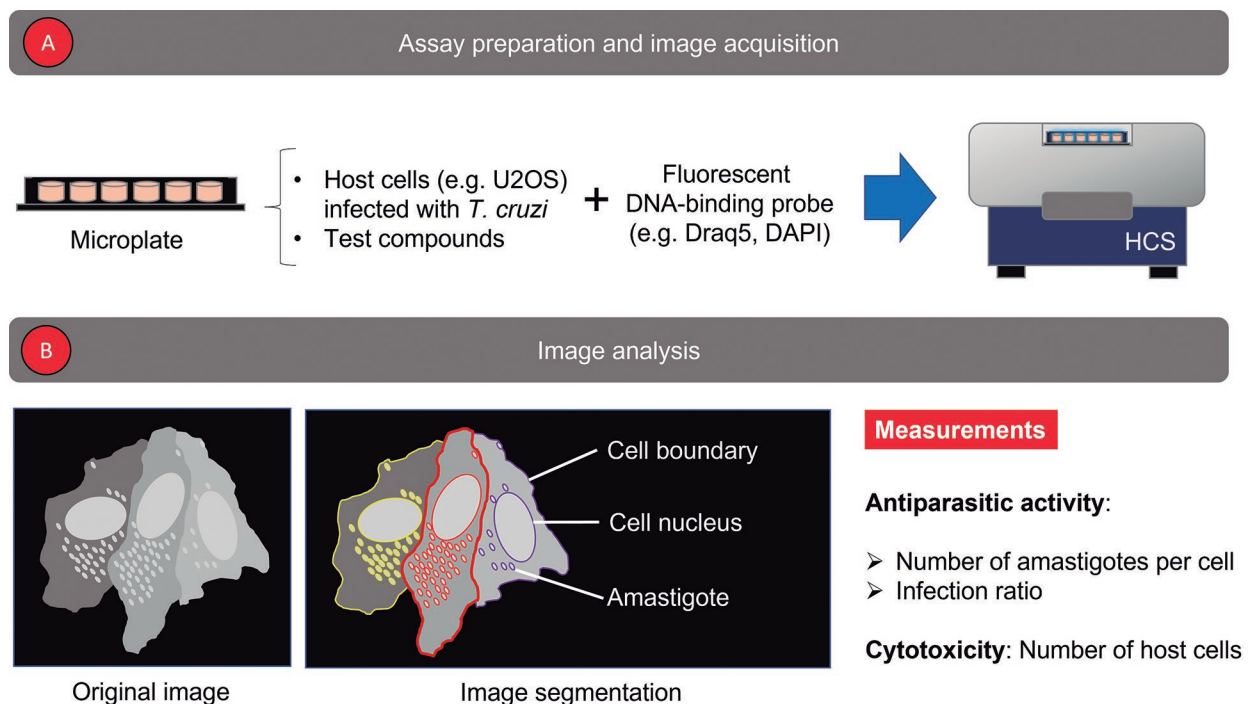


Fig. 3: a single-probe HCS-based intracellular amastigote assay typically used in the search for new anti-*Trypanosoma cruzi* drugs. (A) Initially, the host infected cells treated with test compounds are stained with a fluorescent DNA-binding probe and their images captured by a HCS system. (B) During image analysis, cells and parasites are segmented individually and counted. From this it is possible to calculate at least two metrics related to compounds anti-trypanosomatid activity: number of amastigotes per cell and the percentage of infected cells (infection ratio). In addition, compounds cytotoxicity can be estimated from cells nuclei count.

^(69,73) Additionally, an estimation of compounds' cytotoxicity can be obtained in the same assay by counting the number of host cells (i.e., their nuclei)^(69,77,81,82) (Fig. 3B). In contrast to visual scoring, HCS-based assays are highly objective, accurate and faster, which make them an ideal tool for screening campaigns.⁽²⁵⁾ Therefore, intracellular amastigote-based assays performed in HCS systems can become the new gold standard in trypanosomatid phenotypic screening by combining the necessary biological complexity of microscope-based assays with the high-throughput of microplate readers.

A variety of trypanosomatid species and/or strains have been interrogated in HCS-based assays (Table). Most of the studies with *Trypanosoma* spp. were carried out with strains of *T. cruzi* from different DTUs. Likewise, many strains of both dermatropic and viscerotropic *Leishmania* species have been investigated. In most cases, they consist of laboratory strains which are easily cultivated *in vitro*. Nonetheless, the solely use of these strains demand caution since they may differ from clinical isolates in terms of genotype and phenotype (e.g., drug resistance).^(17,67) Therefore, it is advisable to confirm hit compounds on a panel of clinical isolates and groups of representative strains (e.g., for each DTU).^(17,18,67,70,83)

The selection of a disease-relevant cell host model at the initial stages of the drug discovery pipeline is crucial to reduce the attrition rates with later steps. The HCS-based methods proposed so far for trypanosomatids were developed using primary cells or commercial cell lines from human or other organisms (murine and primate)

sources (Table). Most *T. cruzi* screenings measured the antiparasitic activity of compounds in muscle cells infected with amastigote forms.^(27,60,69,71,84-89) They represent a particularly good model for compound screening since the pathology described in the chronic phase of Chagas disease is mainly related to the presence of *T. cruzi* in these cells and they have a high susceptibility to infection *in vitro*.⁽⁶⁹⁾ Some reports show that compound activity may vary between different cell types suggesting the presence of specific host-parasite interactions.^(27,90) Therefore, it is suggested that a given hit should be tested against multiple cell models to confirm its potential anti-*T. cruzi* activity.⁽²⁷⁾

For *Leishmania* spp., HCS-based drug screening has been carried out with macrophages or macrophage-like cells: primary murine bone-marrow derived macrophages (BMDM) and human acute monocytic leukemia cells (THP-1), a commercial cell line. Macrophages are disease-relevant models since they exert a dual role in leishmaniasis being at the same time the final host cell for parasite proliferation and the effector cell that contributes to clean the infection.⁽⁹¹⁾ Most assays use THP-1 cells instead of primary cells due to several technical and logistic advantages of the former, such as lower cost, ease of cultivation, applicability to large screening campaigns and less ethical restriction.^(77,92) However, they require external chemical stimuli for monocyte to macrophage transformation and show much less biological relevance.^(76,92) In this context, it is advisable to test the compounds in primary cells whenever possible.^(53,92)

Different methods have been proposed to quantify the number of trypanosomatid amastigotes inside the host cell in HCS-based assays (Table). A common approach consists of using a single DNA-binding fluorescent probe (e.g., Draq5) to stain both cells (nuclei and/or cytoplasm) and parasites (DNA spots composed of kDNA and/or nuclear DNA)^(67,68,69,73,83,87,93-95) (Fig. 3). In this strategy, all objects necessary for calculating the antiparasitic activity of a test compound are contained in the same image. During analysis, cell nuclei and parasite DNA spots are distinguished by size and counted. Cell boundaries can be revealed from probes “leakage” into the cytoplasm and/or inferred by computational tools, allowing the determination of the number of parasites per each cell.^(67,82,95,96) These methods are simple, but they may underestimate parasitaemia when parasites are located at the same place or near a cell’s nucleus, as well as detect non-specific stained spots due to the accumulation of host cell RNA in the cytosol.^(25,69,77,78) Moreover, they generally require cell fixation making it impossible to monitor live cells over time which could inform the time-course of drug action.⁽⁹⁷⁾ The use of computer algorithms to delineate cell boundaries based on nucleus position may also be prone to errors since they often consider that the nucleus is located at the centre of each cell.^(82,96) This may not be true specially for primary cells once their morphology is not as homogeneous as that observed for cell lineages.^(58,77) Therefore, some authors have proposed more elaborated assays using multiple fluorescent probes, cells/parasites carrying reporter genes or immunostaining to better define each image object. The former strategy includes, per instance, the combination of a DNA binding probe (e.g., DAPI) to detect the parasite and another probe to stain the whole host cell or its cytoplasm (e.g., CellMask™ dyes).^(58,78,79,98,99) Recently, transgenic parasites expressing reporter genes (e.g., GFP and mCherry) have also been employed in HCS-based assays and represent a useful way to facilitate their identification in the images and reduce assay cost.^(12,60,74,75,84,97,100) However, this approach has some important drawbacks. One of them is that the parasite carrying this gene is no longer wild-type, which may affect its drug response and its interaction with the host cell.^(12,58,100) Moreover, the technique used to incorporate it into the parasite must be performed for each new species or strain (e.g., a clinical isolate).⁽⁵⁸⁾ Another approach consists in using immunostaining to detect the parasite,⁽⁷⁵⁾ the host cell⁽⁷¹⁾ or both.⁽⁷⁷⁾ In this technique, one or more (e.g., immune serum⁽⁷⁵⁾) antibodies directly bind to parasites/cell antigen(s), whereas a fluorescent-conjugated secondary antibody binds to the antigen-antibody complex allowing its detection. This strategy allows the use of the same image analysis protocol regardless of the parasite strain though it tends to be more time-consuming.⁽⁷⁷⁾

Apart from infection-related metrics, HCS-based assays may also provide other valuable information about the effect of test compounds on the parasite-host interaction. Depending on the probe(s) used to stain the biological sample it is possible to extract and quantify a variety of phenotypic features from image objects, including whole organisms (i.e., host cells⁽⁵³⁾ and parasites⁽⁶⁰⁾) and/or subcellular compartments (e.g., cell nuclei,⁽⁸⁹⁾

kDNA,⁽⁸⁰⁾ pharmacophores vacuoles,⁽⁷⁶⁾ cytoskeleton⁽⁷¹⁾) Certain features, such as those related to morphology (e.g., area, shape) may be altered in the presence of the compound, giving a more detailed description of its antiparasitic and/or cytotoxicity activities.^(71,76,80) Sometimes the alterations are not necessarily associated with morphological changes or be detectable by the probes available. In this case, the use of stains that are sensitive to parasite/cell metabolic activity may be useful as they are not constrained to a specific mechanism. As listed in Table, only two dyes have been successfully employed to detect viable trypanosomatids in HCS-based assays: CFDA-SE⁽⁸⁰⁾ (bloodstream *T. brucei*) and CellTracker Orange CMRA⁽⁷⁸⁾ (promastigote and amastigote of *L. mexicana*). In contrast, there are several viability assays, such as those designed for plate-readers (previously discussed in the text), that could be used as orthogonal methods for this kind of analysis.

Successful examples of HCS-based assays in trypanosomatid screening campaigns - Table shows several examples of HCS-based methods in trypanosomatid drug discovery. Some of them helped to reveal the antiparasitic activity of compounds in screening campaigns (Fig. 4). Bernatchez and colleagues,⁽⁸⁵⁾ for instance, performed a primary screen of 7,680 compounds with confirmed clinical safety (ReFRAME library) on cells infected with *T. cruzi* amastigotes using a HCS-based assay. This technique allowed the identification of seven molecules with potent antiparasitic activity (EC₅₀ values: 0.44 to 480 nM) and high selectivity index (≥ 10). One of the most promising compounds for drug development was 348U87 (**8**) (EC₅₀: 0.63 nM and selectivity index: 1294), a small molecule with antiherpetic properties. Apart from primary screening, HCS technology has also been used in orthogonal/secondary assays.^(60,68,84) Peña and colleagues⁽⁶⁰⁾ employed an interdisciplinary approach to detect potential anti-trypanosomatid agents in a 1.8 mi proprietary compounds (GlaxoSmithKline) library. The primary screening was carried out with microplate-based fluorometric assays using axenic (*L. donovani*) and intracellular (*T. cruzi*) amastigotes, as well as bloodstream (*T. brucei*) parasite forms. The resulting hits followed different paths in the drug discovery pipeline according to the species which included both experimental (e.g., cytotoxicity assay) and computational (e.g., physicochemical filters) steps. For *T. cruzi* and *L. donovani* HCS-based assays were also used to select active compounds against intracellular amastigotes. By the end of the pipeline, three sets (or “boxes”) of compounds with antiparasitic activity and low cytotoxicity were assembled: Leish-BOX (n = 192), Chagas-BOX (n = 222) and HAT-BOX (n = 192), which are provided as an open source for lead discovery programmes.

Though most assays use only one combination of parasite and host cell types, there are some exceptions.^(27,77,83,89) Franco and colleagues,⁽²⁷⁾ for instance, conducted a primary screening consisting of four parallel HCS-based assays, one per host cell lineage. In each assay, 1,280 pharmacologically active compounds (LOPAC library, Sigma-Aldrich) were tested against cells infected with intracellular amastigotes of *T. cruzi* Y-H10 strain, yield-

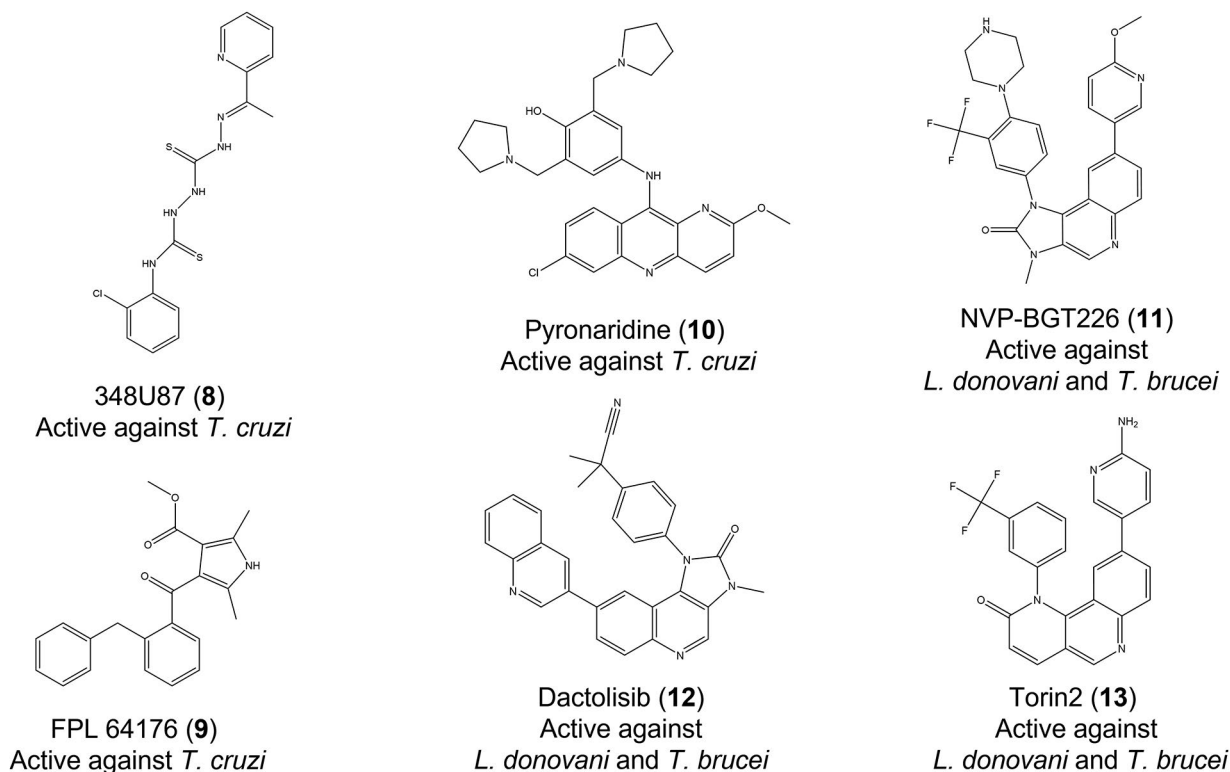


Fig. 4: compounds with anti-trypanosomatid activity identified in screening campaigns that used HCS-based assays.

ing 82 unique hits. The compounds that were active in at least three cell lineages ($n = 11$) had their EC_{50} values calculated, which in most cases were at low micromolar range or lower. One of these compounds, FPL 64176 (9), a Ca^{2+} activator, was active on all four cell line models and showed a similar potency (2.2 - 3.0 μM) across three parasite strains (Y-H10, Sylvio X10/1 and CL Brener), as well as good selectivity indexes (57.7, 35.4 and > 90 , respectively) in U2OS cells.

A few reports have also validated the *in vitro* activity of test compounds on *in vivo* disease models.^(87,88,95) Ekins and colleagues⁽⁸⁷⁾ measured the anti-trypanosomatid activity of commercial compounds combining computational and experimental techniques. Initially, they trained bayesian machine learning models to identify compounds with potential anti-*T. cruzi* *in vitro* activity. These models were then used to screen approximately 7,200 small molecules available in different chemical libraries (mostly from commercial sources). The 97 virtual hits with the highest scores were evaluated in a HCS-based assay that measured their antiparasitic activity and host cell toxicity. Dose-response curves revealed that five of them had an EC_{50} lower than 1 μM . Later, they had their *in vivo* efficacy determined using an acute Chagas mouse model. One of these compounds, pyronaridine (10) (antimalarial drug), had never been tested in a mouse model and showed a high efficacy (85.2 %) when compared to benznidazole (1) (100%). Some potential targets were predicted for this compound using different computational resources, including the *T. cruzi* pathway model

developed in the same study. These results suggested that pyronaridine (10) may be a promising starting point for drug development. Phan and colleagues⁽⁹⁵⁾ also obtained antiparasitic compounds with *in vitro* and *in vivo* activity against *L. donovani* and *T. brucei*. A primary screening of 1,742 commercial bioactive compounds (MedChem Express) was performed with a HCS-based assay using cells infected with intracellular amastigotes of *L. donovani*. This technique revealed 20 molecules with high antileishmanial activity and low cytotoxicity. Some of them were identified as inhibitors of the mammalian target of rapamycin (mTOR)/phosphoinositide 3-kinase (PI3K) (mTOR/PI3K) signaling pathway and had their EC_{50} values determined (0.14 - 13.44 μM). The three most potent molecules (NVP-BGT226 (11), dactolisib (12) and Torin2 (13)) were tested *in vivo* using a mouse model infected with *L. donovani*. They all inhibited parasitaemia in mice, especially NVP-BGT226 (11) (54 % inhibition). This compound also showed anti-*T. brucei* *in vitro* activity (resazurin-based assay) and reduced parasitaemia in a *T. brucei* infected mice model suggesting a broad anti-trypanosomatid effect. However, further studies may be necessary to increase their selectivity as mTOR and kinetoplastid TORs show high structural similarities and mTOR/PI3K inhibitors have already shown toxicity in clinical trials.

An HCS-centered ideal assay cascade for antileishmanial phenotypic drug screening - In screening campaigns, it is important to balance reliability and pragmatism (Fig. 5). Therefore, the use of *L. amazonensis* as a

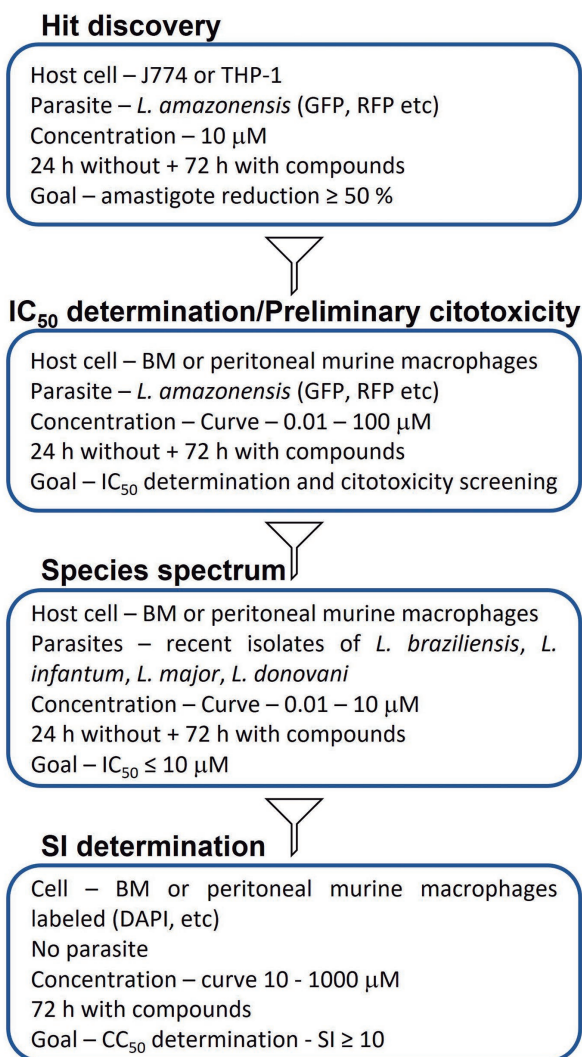


Fig. 5: HCS-centered ideal assay cascade for antileishmanial phenotypic drug screening.

starting point is suggested, due to its rapid growth and high infectivity rate. Ideally, the reporter gene is integrated into the parasite's DNA, to reduce some interference, such as variation in the number of plasmids per cell, or even the lack of it. In the hit discovery step, the use of cell lines such as J774 or THP-1 is acceptable to reduce the number of animals. However, at later stages, primary cells are recommended.⁽⁹²⁾ Still considering pragmatism, the first round using only one concentration reduces resources and improves yield. Here, we adopted the limit of 10 μ M, as recommended as a hit criterion by an expert panel.⁽¹⁰⁶⁾ Another relevant point is to keep cells untreated for up to 24 hours after infection, to ensure complete transformation of promastigotes into amastigotes. Otherwise, the compounds can act on any remaining target of the promastigote. An advantage of the HCS is the possibility of obtaining cytotoxicity data together with the IC₅₀ determination, allowing the disposal of toxic candidates early in the process. At later stages, it becomes neces-

sary to use more clinically relevant *Leishmania* species, as well as to determine the CC₅₀ in primary uninfected cells, before going to in vivo assays.

Final remarks - As discussed here, automated, image-based screening approaches known as HCS, have already made a major impact in trypanosomatid drug discovery and hold the promise to keep occupying an important space in the field for the years to come. This is so because HCS has several advantages over non image-based HTS including acquisition of multidimensional (2D and 3D) data, multiplexing capacity and multiparametric analysis for phenotypic scoring.

Even with the technological advantages of HCS, it's key for the success of a trypanosomatid drug screening campaign to use carefully standardised reagents and optimised assays parameters. Compound-parasite incubation times and the sequential cell and compound seeding schemes have already been demonstrated as crucial factors that can be responsible for apparent lack of activity of compounds in a particular assay setup.⁽¹⁰⁷⁾ Moreover, as a high-throughput experimental method, HCS presents a number of intrinsic challenges such as: experimental design errors, high cost and availability of materials (cells, proteins, compounds, etc.); compounds and reagents-related issues (incorrect structures, mixtures and salts, inconsistent batches, poor solubility); and other technical problems (pipetting errors and mechanical failures, temperature gradients, position effects, suboptimal readings). For instance, frequent hitter compounds (aggregators, interferers, etc.) may lead to false positives in screening campaigns and failure to validate initial hits on secondary assays.^(108,109)

A better understanding of the host/parasite interaction and the disease itself is essential if we are to be able to design better and more predictive phenotypic assays. For instance, there are still unanswered questions regarding cell dormancy in *T. cruzi*: do we need assays targeting replicating and non-replicating forms of parasites?

A combination of phenotypic and target-based drug discovery approaches should lead to better chances of identifying compounds with the potential to satisfy the target product profile (TPP) of diseases caused by trypanosomatids. Additionally, the integration of machine learning and other AI or computational modeling techniques should help to make the most efficient use of resources.

Finally, incorporating newly developed assays into the phenotypic screening cascade is an exciting perspective to the field. Exploration of novel genetic editing methods, such as CRISPR/Cas9,⁽¹¹⁰⁾ allows creation of dual or even triple reporter systems for *in vitro* and *in vivo* multimodal imaging.^(110,111) These parasite cell lines enable efficient *in vivo* localisation and phenotyping, expanding the toolbox for trypanosomatid drug discovery.

AUTHORS' CONTRIBUTION

FPSJr designed the manuscript, wrote the abstract, final remarks and reviewed the first draft; RFD wrote the first draft and reviewed the HCS-based assays used in trypanosomatid drug discovery; ECTS wrote the assay cascade session and reviewed the first draft.

TABLE
HCS-based assays employed in trypanosomatid drug discovery

Genus	Species	Strains	Evolutionary forms	Reporter	Host cell	Main measurements	Assay principle	Screened compounds	Pipeline step	References
<i>Trypanosoma</i>	<i>T. brucei brucei</i> (wild type and genetically engineered kDNA-independent cell lines) ⁽⁶⁰⁾	Laboratory strain: Lister-427	Bloodstream	None	-	kDNA/nucleus ratio	Parasite nuclear DNA and kDNA detected by Hoechst 33342 while viable parasites by CFDA-SE	13,486 compounds from three commercial libraries (Prestwick Chemical Library, Screen-Well PKC library and BioAssent 12,000 diverse chemical libraries)	Primary screening	⁽⁶⁰⁾
		Laboratory strain: Y	Intracellular amastigotes	None	Human induced pluripotent stem cell-derived cardiomyocytes (hiPSC-CM)	Number of host cells (lethal cytotoxicity evaluation), number of amastigotes per cell, infection rate and sublethal cytotoxicity-related parameters	Screening: Parasites DNA spots and cell nucleus detected by Draq5 while cell cytoplasm by cFNT immunostaining; Cytotoxicity assay: Cell nucleus, cytoskeleton and mitochondria detected by DAPI, Phalloidin-488 and MitoTracker™ Red, respectively	4 compounds with known anti-trypanosomatid activity	Primary screening (dose-response) and cytotoxicity assay	⁽⁷¹⁾
		Laboratory strain: Tulahuén	Intracellular amastigotes	<i>Escherichia coli</i> beta-galactosidase gene ⁽⁶⁴⁾	Rat cardiomyocytes (H9c2)	Number of host cells (cytotoxicity evaluation), number of amastigotes per cell and percentage of infected cells per well	Parasites DNA spots as well as cell nucleus and cytoplasm detected by Draq5	20 compounds with known anti-trypanosomatid activity	Primary screening (dose-response) and cytotoxicity evaluation performed in the same assay	⁽⁶⁶⁾
<i>Trypanosoma</i>	<i>T. cruzi</i>	Laboratory strain: Tulahuén	Intracellular amastigotes	None	Mouse embryo fibroblast (3T3)	Number of amastigotes per cell and number of infected cells per well	Parasites DNA spots and cell nucleus detected with Hoechst 33342 while cell cytoplasm with HCS CellMask Green™	741 compounds (FDA-approved and with biological activity) from a in-house library and 685 compounds from a pilot collection of Medicines for Malaria Venture Malaria Box	Primary screening and dose-response assay	⁽⁷⁰⁾
		Laboratory strain: Tulahuén	Intracellular amastigotes	None	Mouse embryo fibroblast (3T3)	Number of host cells (cytotoxicity evaluation), number of amastigotes per cell and number of infected cells per well	Parasites DNA spots and cell nucleus detected with Hoechst 33342; Proliferation assay: EdU incorporation by parasites (trypanosomites and amastigotes) and cell nucleus detected by Click-iT Plus EdU Alexa-Fluor 488 Imaging Kit.	24,993 compounds optimised for lead-like properties	Primary screening and cytotoxicity evaluation performed in the same assay. A similar method was used to generate the dose-response curves and for further profiling of selectively active compounds. Protocol based on a previous report ⁽⁷²⁾ . A wash-off assay was also carried out by HCS.	⁽⁷²⁾
		Laboratory strains: Silvio X10/7 subclone A1, Y, M6241 Clone 6, ERA Clone 2, PAH179 Clone 5, Tula Clone 2 and CL Brener.	Trypomastigotes and intracellular amastigotes	CL Brener strain carrying a gene reporter (red-shifted luciferase) ⁽⁶⁵⁾	<i>Cercophithecus aesthiops</i> kidney cell (Vero)	Number of host cells (cytotoxicity evaluation), number of amastigotes per cell, number of amastigotes per well, percentage of infected cells and percentage of EdU (nucleoside analog) positive cells and parasites	Primary screening and replication assay (amastigotes); parasites DNA spots as well as cell nucleus and cytoplasm detected by Hoechst 33342; Proliferation assay: EdU incorporation by parasites (trypanosomites and amastigotes) and cell nucleus detected by Click-iT Plus EdU Alexa-Fluor 488 Imaging Kit. Trypomastigote flagellum was also detected by immunostaining (anti-PFRI antibody)	3 trypanocidal drugs	Primary screening (dose-response) and cytotoxicity evaluation performed in the same assay. Replication and proliferation assays were also carried out using a HCS system. Protocol based on a previous report ⁽⁶⁴⁾ .	⁽⁷³⁾



Genus	Species	Strains	Evolutionary forms	Reporter	Host cell	Main measurements	Assay principle	Screened compounds	Pipeline step	References
		Not declared	Intracellular amastigotes	None	Human osteosarcoma cells (U2OS)	Number of host cells (cytotoxicity evaluation), number of amastigotes per cell and infection ratio	Parasites DNA spots as well as cell nucleus and cytoplasm detected by Draq5	2 trypanocidal drugs	Primary screening (dose-response) and cytotoxicity evaluation in the same assay	(60)
		Laboratory strains: Dm28c, Y, ARMA13 cl1, ERA cl2, 92-80 cl2, CL Brener and Tlilähnen	Intracellular amastigotes	None	Human osteosarcoma cells (U2OS)	Number of amastigotes per cell and infection ratio	Parasites DNA spots as well as cell nucleus and cytoplasm detected by Draq5	8 lead/clinical compounds with anti-trypanosomatid activity	Primary screening (dose-response) and time-kill assay. Protocols based on a previous report ⁽⁶⁰⁾ .	(70)
		Laboratory strain: Y	Intracellular amastigotes	None	Human osteosarcoma cells (U2OS)	Number of host cells (cytotoxicity evaluation), number of amastigotes per cell and infection ratio	Parasites DNA spots as well as cell nucleus and cytoplasm detected by Draq5	39 commercial compounds selected from a virtual screening of the ChemBridge chemical database (1 M compounds)	Primary screening (dose-response) and cytotoxicity evaluation performed in the same assay. Protocol based on a previous report ⁽⁷⁰⁾ .	(81)
		Laboratory strains: Y-H10, Sylvio X10/1 and CL Brener	Intracellular amastigotes	None	Human osteosarcoma cells (U2OS), human acute monocytic leukemia (THP-1) cells, <i>Cercophithecus aethiops</i> kidney cell (Vero) and rat skeletal myoblast (L6) cells	Number of host cells (cytotoxicity evaluation), number of amastigotes per cell and infection ratio	Parasites DNA spots as well as cells nucleus and cytoplasm detected by Draq5	1,280 compounds from LOPAC library (Sigma-Aldrich)	Primary screening and cytotoxicity evaluation performed in the same assay using Y-H10 strain. Similar method was employed to dose-response curves. Protocol based on a previous report ⁽⁶⁵⁾ .	(27)
		Laboratory strains: Y	Intracellular amastigotes	None	Human osteosarcoma cells (U2OS)	Number of host cells (cytotoxicity evaluation) and infection ratio	Parasites DNA spots as well as cell nucleus and cytoplasm detected by Draq5	24 novel compounds derived from farnesyltransferase inhibitors	Primary screening (dose-response) and cytotoxicity evaluation performed in the same assay. Protocol based on a previous report ⁽⁷⁰⁾ .	(69)
		Laboratory strains: Y	Intracellular amastigotes	None	Murine fibroblasts (NIH 3T3) expressing GFP	Number of amastigotes per cell and percentage of infected cells	Parasites DNA spots and cells nucleus detected by DAPI while cell body detected by GFP	21 treatment groups from an on-going study	Primary screening	(25)
		Laboratory strain: CA-1/72	Intracellular amastigotes	None	Mouse myoblasts (C2C12)	Number of host cells (cytotoxicity evaluation) and infection level (number of amastigotes per cell as determined by nuclei counting)	Parasites DNA spots and cells nucleus detected by DAPI	7,680 compounds from RefFRAME library	Primary screening and cytotoxicity evaluation performed in the same assay. A similar method was used to generate the dose-response curves. Protocol based on previous reports ^(68,67,66) .	(85)
		Laboratory strains: CA-1/72	Intracellular amastigotes	None	Mouse myoblasts (C2C12)	Number of host cells (cytotoxicity evaluation) and infection level (number of amastigotes per cell)	Parasites DNA spots and cells nucleus detected by DAPI	Gallinamide A and 15 analogs	Primary screening (dose-response) and cytotoxic evaluation performed in the same assay. Protocol based on a previous report ⁽⁸⁷⁾ .	(86)
		Laboratory strain: CA-1/72	Intracellular amastigotes	None	Mouse myoblasts (C2C12)	Number of host cells (cytotoxicity evaluation) and infection ratio	Parasites DNA spots and cell nucleus detected by DAPI	97 commercial compounds selected by virtual screening	Primary screening and cytotoxicity evaluation performed in the same assay. A similar method was used to generate the dose-response curves	(87)

Trypanosoma



Genus	Species	Strains	Evolutionary forms	Reporter	Host cell	Main measurements	Assay principle	Screened compounds	Pipeline step	References
		Laboratory strain: Silvio X10/7 A1	Intracellular amastigotes	None	<i>Cercopithecus aethiops</i> kidney cells (Vero)	Number of host cells (cytotoxicity evaluation), number of amastigotes per cell and percentage of infected cells	Parasites DNA spots as well as cell nucleus and cytoplasm detected by Hoechst 33342	14,080 commercial compounds from NIH (clinical collection) and Selleck-Chem (FDA-approved drug library) libraries	Primary screening and cytotoxicity evaluation performed in the same assay. Similar methods were used to dose-response, cell replication, static-cidal and rate-of-kill assays. Protocols based on previous reports ^(65,66,69) .	(64)
		Laboratory strains: CA-172, PSD-1 and Sylvio X10/7	Intracellular amastigotes	None	Bovine embryo skeletal muscle (BESM) and human hepatoma (Huh-7) cells	Number of host cells (cytotoxicity evaluation) and kDNA/host nuclei ratio	Parasites kDNA and cell nucleus detected by DAPI	909 clinical compounds library from Iconix Biosciences	Primary screening and cytotoxicity evaluation performed in the same assay. A similar method was used to generate the dose-response curves	(68)
		Laboratory strain: CA-172	Intracellular amastigotes	None	Mouse myoblasts (C2C12)	Number of host cells (cytotoxicity evaluation), infection ratio and area of infection (area of kinetoplasts/total nuclei)	Parasites DNA spots and cell nucleus detected by DAPI, cell body inferred by aggregating parasites DNA spots and cell nucleus image objects	180,329 compounds from GNF Academic Collaboration Library	Primary screening and cytotoxicity evaluation performed in the same assay. A similar method was used to generate the dose-response curves. Protocols based on a previous report ⁽⁶⁶⁾	(68)
		Laboratory strain: Tulahuen	Intracellular amastigotes	<i>Escherichia coli</i> β -galactosidase gene ⁽⁶⁴⁾	Rat cardiomyocytes (H9c2)	Number of host cells (cytotoxicity evaluation), number of amastigotes per cell and infection ratio	Parasites DNA spots as well as cell nucleus and cytoplasm detected by Draq5	2,310 compounds from GlaxoSmithKline HTS screening collection	Orthogonal assay (screening and cytotoxicity evaluation). Protocol based on a previous report ⁽⁶⁶⁾	(66)
		Laboratory strain: STIB980 clone 1	Intracellular amastigotes	eGFP	Peritoneal mouse macrophages	Number of host cells (cytotoxicity evaluation), number of amastigotes per image and fold change in parasite numbers per hour	Parasite kDNA and cell nucleus detected by Hoechst 33342. Parasites also identified by GFP staining in live imaging assay	2 anti-trypanosomatid drugs	Secondary assay (dose-response and cytotoxicity evaluation)	(67)
		Laboratory strain: Tulahuen	Intracellular amastigotes	<i>Escherichia coli</i> β -galactosidase gene ⁽⁶⁴⁾	Rat cardiomyocytes (H9c2)	Number of host cells (cytotoxicity evaluation), number of amastigotes per cell and infection ratio	Parasites DNA spots as well as cell nucleus and cytoplasm detected by Draq5	3,598 compounds from Calibr Diversity Library	Secondary assay (screening and cytotoxicity evaluation) and dose-response assay. Protocol based on previous reports ^(66,69)	(64)
		Laboratory strain: Talahuen	Intracellular amastigotes	GFP ⁽⁶³⁾	Monkey kidney epithelial (LLCMK2) cells	Number of intracellular amastigotes per well	Cells nucleus detected by DAPI and amastigotes by GFP staining	4 phenothiazinium dyes	Primary screening (dose-response)	(64)
		Laboratory strain: Tulahuen	Intracellular amastigotes	None	Mouse embryo fibroblasts (3T3)	Number of amastigotes per cell and number of infected host cells per well	Parasites DNA spots and cell nucleus detected by Hoechst 33342 while cell cytoplasm by HCS CellMask Green™	472 compounds from Davis open access natural product-based library	Primary screening and dose-response assay. Protocol based on a previous report ⁽⁷⁰⁾	(66)
		Laboratory strains: <i>L. donovani</i> (MHOM/IN/1980/DD8), <i>L. amazonensis</i> (MHOM/BR/1971/LTB0016) and <i>L. braziliensis</i> (MHOM/BR/1975/M2903)	Intracellular amastigotes	None	Human acute monocytic leukemia (THP-1) cells	Number of host cells (cytotoxicity evaluation), number of amastigotes per cell and infection ratio	Parasites DNA spots as well as cell nucleus and cytoplasm detected by Draq5	1,280 compounds from LOPAC library	Primary screening and cytotoxicity evaluation performed in the same assay. A similar method was used to generate the dose-response curves. Protocol based on a previous report ⁽⁶²⁾	(68)
<i>Trypanosoma</i>										
	<i>Leishmania</i>									



Genus	Species	Strains	Evolutionary forms	Reporter	Host cell	Main measurements	Assay principle	Screened compounds	Pipeline step	References
<i>L. donovani</i>	<i>L. donovani</i>	Laboratory strain: MHOM/SD/62/ISCL2D, LdBOB	Intracellular amastigotes	GFP ⁽⁵³⁾	Human acute monocytic leukemia cells (THP-1)	Number of amastigotes per cell, infection ratio and number of parasites labeled with EDU	Cell nucleus and cytoplasm detected by DAPI while amastigotes by GFP staining. In the proliferation assay the incorporation of EDU in newly synthesized DNA was measured using Click-IT™ Plus Alexa Fluor™ 647 Picolyl Azide Toolkit	2 antileishmanial drugs	Primary screening (dose-response) and proliferation assay. Protocol based on previous reports ^(53,60)	(74)
		Laboratory strain: MHOM/SD/62/IS-cl2D	Intracellular amastigotes	None	Human acute monocytic leukemia (THP-1) cells	Number of host cells (cytotoxicity evaluation) and number of amastigotes per cell	Parasites kDNA and cell nucleus detected by DAPI. Cell boundary was delineated around the nucleus object	909 bioactive compounds library from Iconix Biosciences	Primary screening and cytotoxicity evaluation performed in the same assay. A similar method was used to generate the dose-response curves	(66)
		Laboratory strains: <i>L. donovani</i> (MHOM/ET/67/HU3), <i>L. amazonensis</i> (MHOM/BR/73/M2269), <i>L. braziliensis</i> (MHOM/BR/2903) and <i>L. major</i> (MHOM/IL/81/FRIEDLIN)	Intracellular amastigotes	None	Human acute monocytic leukemia cells (THP-1)	Number of host cells (cytotoxicity evaluation), number of amastigotes per cell and infection ratio	Parasites DNA spots and cell nucleus detected by Draq5. Individual cells were segmented after a series of computational tasks that use the nucleus as a seed point	4 antileishmanial drugs	Primary screening (dose-response) and cytotoxicity evaluation performed in the same assay	(82)
<i>Leishmania</i>	<i>L. donovani</i> and <i>L. major</i>	Laboratory strains: <i>L. donovani</i> (MHOM/ET/67/HU3) and <i>L. major</i> (MHOM/IL/81/FRIEDLIN)	Intracellular amastigotes	None	Human acute monocytic leukemia cells (THP-1)	Infection ratio	Parasites DNA spots as well as cell nucleus and cytoplasm detected by Draq5	124 compounds from TimTec library	Hit confirmation assay (dose-response)	(68)
		Laboratory strain: MHOM/SD/62/IS-CL2D (LdBOB)	Intracellular amastigotes	<i>Aequorea victoria</i> sGFP	Human acute monocytic leukemia cells (THP-1)	Number of host cells (cytotoxicity evaluation), number of amastigotes per cell and number of infected cells	Cell nucleus and body detected by DAPI and HCS Cellmask™ Deep Red, respectively. Parasites detected by GFP staining	15,659 diverse compounds library	Primary screening and cytotoxicity evaluation performed in the same assay. A similar method was used to generate the dose-response curves	(65)
<i>L. infantum</i> and <i>L. amazonensis</i>	LRV1-containing <i>L. guyanensis</i>	Laboratory strain: MHOM/BR/75/M4147	Intracellular amastigotes	None	Primary murine bone-marrow derived macrophages	Number of host cells (cytotoxicity evaluation) and number of amastigotes per cell	Parasites DNA spots and cells nucleus detected by DAPI while cell cytoskeleton (cytosol) by phalloidin-Alexa488	1,520 compounds from Prestwick Chemical Library	Primary screening and cytotoxicity evaluation performed in the same assay. A similar method was used to generate the dose-response curves. Protocol based on a previous report ⁽⁶⁾	(67)
		Laboratory strains: <i>L. infantum</i> (MHOM/MA/67/ITMAP-2,63) and <i>L. amazonensis</i> (MHOM/BR/LTB0016)	Intracellular amastigotes	None	Primary murine bone-marrow derived macrophages	Number of amastigotes per cell and percentage of infected cells	Parasites DNA spots and cells nucleus detected by DAPI while cell body by CellMask™ Deep Red	1 antileishmanial drug	Primary screening (dose-response). Protocol based on previous reports ^(61,52,89)	(68)



Genus	Species	Strains	Evolutionary forms	Reporter	Host cell	Main measurements	Assay principle	Screened compounds	Pipeline step	References
	<i>L. donovani</i> and <i>L. amazonensis</i>	Laboratory strains: <i>L. donovani</i> (MHOM/SD/62/IS-CL2D) and <i>L. amazonensis</i> (MPRO/BR/1972/M1841)	Intracellular amastigotes	mCherry (<i>L. amazonensis</i>)	Primary murine bone-marrow derived macrophages	<i>L. donovani</i> : Number of host cells (cytotoxicity evaluation), number of amastigotes per cell and percentage of infected cells; <i>L. amazonensis</i> : Number of amastigotes, number of total host cells (TM, nucleus counting), number of healthy host cells (HM, based on nucleus size and intensity features), number of parasitophorous vacuoles (PV), viability index (HM/TM) and FV/HM ratio	<i>L. donovani</i> assay: parasites DNA spots and cell nucleus detected by Hoechst 33342 while cell body by HCS CellMask™ Blue. Parasites detected by immunostaining using hamster (infected with <i>L. donovani</i>) immune serum and secondary antibody anti-hamster conjugated with Alexa Fluor 488; <i>L. amazonensis</i> assay: cell nucleus, parasitophorous vacuoles and parasites detected by Hoechst 33342, LysoTracker Green DND-26 and mCherry staining, respectively	188 compounds from Leish-Box	Primary screening and cytotoxicity evaluation performed in the same assay (<i>L. donovani</i> and <i>L. amazonensis</i>). A similar method was used to generate the dose-response curves (<i>L. donovani</i>). Protocol based on a previous report ⁽⁷⁵⁾	(75)
<i>Leishmania</i>	<i>L. major</i> , <i>L. donovani</i> and <i>L. infantum</i>	Laboratory strains: <i>L. major</i> (MHOM/SU/73/5ASKH), <i>L. donovani</i> (BPK190), <i>L. infantum</i> (MHOM/FR/91/LEM 2259, belonging to zymodeme MON-1 clone 351) and <i>L. braziliensis</i> (MHOM/PE/01/PER005 cl.2)	Intracellular amastigotes	None	Primary murine bone-marrow derived macrophages	Number of host cells (cytotoxicity evaluation), number of amastigotes per well, number of amastigotes per cell and infection ratio	Cell nucleus detected by DAPI while cell cytoplasm and parasites detected by immunostaining using mouse anti-Hsp90 primary antibody and anti-mouse secondary antibody conjugated with Alexa Fluor 647	6 immunostimulatory <i>Ethp1b</i> -compounds	Primary screening (dose-response) and cytotoxicity evaluation performed in the same assay	(77)
	<i>L. amazonensis</i>	LV79 (MPRO/BR/1972/M1841)	Intracellular amastigotes	DsRed2 ⁽⁶⁸⁾	Primary murine bone-marrow derived macrophages	Number of amastigotes, number of total host cells (TM, nucleus counting), number of healthy host cells (HM, based on nucleus size and intensity features), number of parasitophorous vacuoles (PV), viability index (HM/TM) and PV/HM ratio	Cell nucleus, parasitophorous vacuoles and parasites detected by Hoechst 33342, LysoTracker Green DND-26 and DsRed2 staining, respectively	60 compounds with established or potential leishmanicidal, antifungal or antimicrobial and cytotoxic activities	Primary screening and cytotoxicity evaluation performed in the same assay. A similar method was used to generate the dose-response curves	(76)
	<i>L. mexicana</i>	MNYC/BZ/62/M379	Intracellular amastigotes	None	Human acute monocytic leukemia cells (THP-1)	Number of host cells (cytotoxicity evaluation), average number of amastigotes per cell and frequency distribution of intracellular amastigotes	Parasites detected by CellTracker™ Orange CMRA while cell body and nucleus detected by CellTracker™ Green CMFDA and DAPI, respectively	3 antileishmanial drugs	Primary screening (dose-response) and cytotoxicity evaluation performed in the same assay	(78)
	<i>L. donovani</i>	Recent clinical isolates sensitive and resistant to pentavalent antimonials (SSG); SSG-sensitive (MHOM/NP/03/BPK282/0 clone 4) and SSG-resistant (MHOM/NP/03/BPK275/0 clone 18)	Intracellular amastigotes	None	Human acute monocytic leukemia cells (THP-1)	Number of amastigotes per cell and infection ratio	Parasites DNA spots as well as cells nucleus and cytoplasm detected by Draq5	130 compounds from Leish-box (GSK)	Primary screening (dose-response). Protocol based on previous reports ^(53,60)	(67)



Genus	Species	Strains	Evolutionary forms	Reporter	Host cell	Main measurements	Assay principle	Screened compounds	Pipeline step	References
<i>L. donovani</i>	<i>L. donovani</i>	Laboratory strain: MHOM/SD/62/IS-CL2D	Intracellular amastigotes	None	Human acute monocytic leukemia cells (THP-1)	Number of host cells (cytotoxicity evaluation), number of amastigotes per cell and infection ratio	Parasites DNA spots as well as cell nucleus and cytoplasm detected by Draq5	1,742 bioactive compounds from MedChem Express	Primary screening and cytotoxicity evaluation performed in the same assay. A similar method was used to generate the dose-response curves. Protocol based on a previous report ⁽⁶⁵⁾	(65)
		Laboratory strain: MHOM/SD/62/IS-CL2D, LdBOB	Intracellular amastigotes	<i>Aequorea victoria</i> eGFP	Human acute monocytic leukemia cells (THP-1)	Number of host cells (cytotoxicity evaluation), number of amastigotes per cell and infection ratio	Cell nucleus and cytoplasm detected by DAPI while parasites by GFP staining	32,700 compounds from GlaxoSmithKline HTS screening collection	Secondary screening and dose-response assay (also cytotoxicity evaluation). Protocol based on previous reports ^(65,70)	(66)
		Laboratory strain: MHOM/SD/62/IS-CL2D, LdBOB	Intracellular amastigotes	<i>Aequorea victoria</i> eGFP	Human acute monocytic leukemia cells (THP-1)	Number of host cells (cytotoxicity evaluation), number of amastigotes per cell and infection ratio	Cell nucleus and cytoplasm detected by DAPI while parasites by GFP staining	1,392 compounds from Diversity Library from Calibr	Secondary screening and cytotoxicity evaluation performed in the same assay. A similar method was used to generate the dose-response curves. Protocol based on previous reports ^(65,70)	(64)
<i>Leishmania</i>	<i>L. donovani</i>	Laboratory strain: MHOM/IN/80 DD8	Intracellular amastigotes	None	Human acute monocytic leukemia cells (THP-1)	Number of amastigotes per cell and number of infected cells normalized to the positive and negative controls	Parasites DNA spots detected by SYBR green while cell body and nucleus by CellMask™ Deep Red and SYBR green, respectively	472 natural product-derived library from Davis open access	Primary screening and dose-response assay. Protocol based on a previous report ⁽⁶⁹⁾	(68)
		Laboratory strain: MHOM/IN/80 DD8	Intracellular amastigotes	None	Human acute monocytic leukemia cells (THP-1)	Number of amastigotes per cell and number of infected cells normalized to the positive and negative controls	Parasites DNA spots detected by SYBR green while cell body and nucleus by CellMask™ Deep Red and SYBR green, respectively	400 compounds from Medicines for Malaria Venture Pathogen Box	Primary screening and dose-response assay	(69)

CFDA-SE - 5(6)-carboxyfluorescein diacetate succinimidyl ester, CMFDA - 5-chloromethylfluorescein diacetate, cTNT - cardiac troponin-T, DAPI - 4',6-diamidino-2-phenylindole, EdU - 5-ethynyl-2-deoxyuridine, GFP - Green fluorescent protein, GNf - Institute of the Novartis Research Foundation, Hsp90 - 90 kDa heat shock protein, HTS - High throughput screening, kDNA - Kinetoplast DNA, LOPAC - Library of Pharmacologically Active Compounds, LRVI - Leishmania RNA virus 1, PFR1 - paraflagellar rod protein 1, ReFRAME - Repurposing, Focused Rescue, and Accelerated Medchem.

REFERENCES

1. Lukeš J, Butenko A, Hashimi H, Maslov DA, Votýpka J, Yurchenko V. Trypanosomatids are much more than just trypanosomes: clues from the expanded family tree. *Trends Parasitol.* 2018; 34(6): 466-80.
2. Votýpka J, d'Avila-Levy CM, Grellier P, Maslov DA, Lukeš J, Yurchenko V. New approaches to systematics of trypanosomatidae: criteria for taxonomic (re)description. *Trends Parasitol.* 2015; 31(10): 460-9.
3. Kaufer A, Ellis J, Stark D, Barratt J. The evolution of trypanosomatid taxonomy. *Parasit Vectors.* 2017; 10(1): 287.
4. WHO - World Health Organization. Leishmaniasis [updated 2021; cited 2021 Dec 18]. Health topics. Available from: https://www.who.int/health-topics/leishmaniasis#tab=tab_1.
5. Echeverria LE, Morillo CA. American trypanosomiasis (Chagas disease). *Infect Dis Clin North Am.* 2019; 33(1): 119-34.
6. Vela A, Coral-Almeida M, Sereno D, Costales JA, Barnabé C, Brenière SF. *In vitro* susceptibility of *Trypanosoma cruzi* discrete typing units (DTUs) to benznidazole: a systematic review and meta-analysis. *PLoS Negl Trop Dis.* 2021; 15(3): e0009269.
7. Messenger LA, Miles MA, Bern C. Between a bug and a hard place: *Trypanosoma cruzi* genetic diversity and the clinical outcomes of Chagas disease. *Expert Rev Anti Infect Ther.* 2015; 13(8): 995-1029.
8. Nielebock MAP, Moreira OC, Xavier SCC, Miranda LFC, Lima ACB, Pereira TOJS, et al. Association between *Trypanosoma cruzi* DTU TeII and chronic Chagas disease clinical presentation and outcome in an urban cohort in Brazil. *PLoS One.* 2020; 15(12): e0243008.
9. de Oliveira MT, Sulleiro E, da Silva MC, Silgado A, de Lana M, da Silva JS, et al. Intra-discrete typing unit TeV genetic variability of *Trypanosoma cruzi* in Chronic Chagas' disease Bolivian immigrant patients in Barcelona, Spain. *Front Cardiovasc Med.* 2021; 8: 665624.
10. Uliana SRB, Trinconi CT, Coelho AC. Chemotherapy of leishmaniasis: present challenges. *Parasitology.* 2018; 145(4): 464-80.
11. WHO - World Health Organization. Leishmaniasis [updated 2021 May 20; cited 2021 Dec 18]. Newsroom. Available from: <https://www.who.int/news-room/fact-sheets/detail/leishmaniasis>.
12. Zulfiqar B, Shelper TB, Avery VM. Leishmaniasis drug discovery: recent progress and challenges in assay development. *Drug Discov Today.* 2017; 22(10): 1516-31.
13. Sasidharan S, Saudagar P. Leishmaniasis: where are we and where are we heading? *Parasitol Res.* 2021; 120(5): 1541-54.
14. CDC - Centers of Disease Control and Prevention. Leishmaniasis [updated 2017 Dec 14; cited 2021 Dec 18]. DPDx - Laboratory identification of parasites of public health concern. Available from: <https://www.cdc.gov/dpdx/leishmaniasis/index.html>.
15. Aronson NE, Joya CA. Cutaneous Leishmaniasis: updates in diagnosis and management. *Infect Dis Clin North Am.* 2019; 33(1): 101-17.
16. Burza S, Croft SL, Boelaert M. Leishmaniasis. *Lancet.* 2018; 392(10151): 951-70.
17. Villalta F, Rachakonda G. Advances in preclinical approaches to Chagas disease drug discovery. *Expert Opin Drug Discov.* 2019; 14(11): 1161-74.
18. Field MC, Horn D, Fairlamb AH, Ferguson MAJ, Gray DW, Read KD, et al. Anti-trypanosomatid drug discovery: an ongoing challenge and a continuing need. *Nat Rev Microbiol.* 2017; 15(4): 217-31.
19. Chatelain E, Ioset J-R. Phenotypic screening approaches for Chagas disease drug discovery. *Expert Opin Drug Discov.* 2018; 13(2): 141-53.
20. Barrias ES, Reignault LC, De Souza W, Carvalho TMU. Dynasore, a dynamin inhibitor, inhibits *Trypanosoma cruzi* entry into peritoneal macrophages. *PLoS One.* 2010; 5(1): e7764.
21. Neal RA, Croft SL. An *in-vitro* system for determining the activity of compounds against the intracellular amastigote form of *Leishmania donovani*. *J Antimicrob Chemother.* 1984; 14(5): 463-75.
22. Berman JD, Lee LS. Activity of antileishmanial agents against amastigotes in human monocyte-derived macrophages and in mouse peritoneal macrophages. *J Parasitol.* 1984; 70(2): 220-5.
23. Atienza J, Martínez-Díaz RA, Gómez-Barrio A, Escario JA, Herrero A, Ochoa C, et al. Activity assays of thiazidine derivatives on *Trichomonas vaginalis* and amastigote forms of *Trypanosoma cruzi*. *Chemotherapy.* 1992; 38(6): 441-6.
24. Fumarola L, Spinelli R, Brandonisio O. *In vitro* assays for evaluation of drug activity against *Leishmania* spp. *Res Microbiol.* 2004; 155(4): 224-30.
25. Nohara LL, Lema C, Bader JO, Aguilera RJ, Almeida IC. High-content imaging for automated determination of host-cell infection rate by the intracellular parasite *Trypanosoma cruzi*. *Parasitol Int.* 2010; 59(4): 565-70.
26. Sereno D, Cordeiro-da-Silva A, Mathieu-Daude F, Ouaisi A. Advances and perspectives in *Leishmania* cell based drug-screening procedures. *Parasitol Int.* 2007; 56(1): 3-7.
27. Franco CH, Alcántara LM, Chatelain E, Freitas-Junior L, Moraes CB. Drug discovery for Chagas disease: impact of different host cell lines on assay performance and hit compound selection. *Trop Med Infect Dis.* 2019; 4(2): 82.
28. Tatipaka HB, Gillespie JR, Chatterjee AK, Norcross NR, Hulverston MA, Ranade RM, et al. Substituted 2-phenylimidazopyridines: a new class of drug leads for human African trypanosomiasis. *J Med Chem.* 2014; 57(3): 828-35.
29. Nühs A, De Rycker M, Manthri S, Comer E, Scherer CA, Schreiber SL, et al. Development and validation of a novel *Leishmania donovani* screening cascade for high-throughput screening using a novel axenic assay with high predictivity of leishmanicidal intracellular activity. *PLoS Negl Trop Dis.* 2015; 9(9): e0004094.
30. Paloque L, Vidal N, Casanova M, Dumètre A, Verhaeghe P, Parzy D, et al. A new, rapid and sensitive bioluminescence assay for drug screening on *Leishmania*. *J Microbiol Methods.* 2013; 95(3): 320-3.
31. Sykes ML, Avery VM. A luciferase based viability assay for ATP detection in 384-well format for high throughput whole cell screening of *Trypanosoma brucei brucei* bloodstream form strain 427. *Parasit Vectors.* 2009; 2(1): 54.
32. Dutta A, Bandyopadhyay S, Mandal C, Chatterjee M. Development of a modified MTT assay for screening antimonial resistant field isolates of Indian visceral leishmaniasis. *Parasitol Int.* 2005; 54(2): 119-22.
33. Rai P, Arya H, Saha S, Kumar D, Bhatt TK. Drug repurposing based novel anti-leishmanial drug screening using *in-silico* and *in-vitro* approaches. *J Biomol Struct Dyn.* 2021: 1-9.
34. Henriques C, Moreira TLB, Maia-Brigagão C, Henriques-Pons A, Carvalho TMU, de Souza W. Tetrazolium salt based methods for high-throughput evaluation of anti-parasite chemotherapy. *Anal Methods.* 2011; 3(9): 2148-55.
35. Bilbao-Ramos P, Sifontes-Rodríguez S, Dea-Ayuela MA, Bolás-Fernández F. A fluorometric method for evaluation of pharmacological activity against intracellular *Leishmania* amastigotes. *J Microbiol Methods.* 2012; 89(1): 8-11.

36. Bowling T, Mercer L, Don R, Jacobs R, Nare B. Application of a resazurin-based high-throughput screening assay for the identification and progression of new treatments for human African trypanosomiasis. *Int J Parasitol Drugs Drug Resist.* 2012; 2: 262-70.
37. Rolón M, Vega C, Escario JA, Gómez-Barrio A. Development of resazurin microtiter assay for drug sensibility testing of *Trypanosoma cruzi* epimastigotes. *Parasitol Res.* 2006; 99: 103-7.
38. Ortiz D, Guiguemde WA, Hammill JT, Carrillo AK, Chen Y, Connelly M, et al. Discovery of novel, orally bioavailable, antileishmanial compounds using phenotypic screening. *PLoS Negl Trop Dis.* 2017; 11(12): e0006157.
39. Faria J, Moraes CB, Song R, Pascoalino BS, Lee N, Siqueira-Neto JL, et al. Drug discovery for human African Trypanosomiasis: identification of novel scaffolds by the newly developed HTS SYBR green assay for *Trypanosoma brucei*. *J Biomol Screen.* 2014; 20: 70-81.
40. Chan MM-Y, Bulinski JC, Chang K-P, Fong D. A microplate assay for *Leishmania amazonensis* promastigotes expressing multimeric green fluorescent protein. *Parasitol Res.* 2003; 89(4): 266-71.
41. Okuno T, Goto Y, Matsumoto Y, Otsuka H, Matsumoto Y. Applications of recombinant *Leishmania amazonensis* expressing egfp or the beta-galactosidase gene for drug screening and histopathological analysis. *Exp Anim.* 2003; 52(2): 109-18.
42. Kessler RL, Gradia DF, Rampazzo RCP, Lourenço ÉE, Fidêncio NJ, Manhaes L, et al. Stage-regulated GFP expression in *Trypanosoma cruzi*: applications from host-parasite interactions to drug screening. *PLoS One.* 2013; 8(6): e67441.
43. Corman HN, Shoue DA, Norris-Mullins B, Melancon BJ, Morales MA, McDowell MA. Development of a target-free high-throughput screening platform for the discovery of antileishmanial compounds. *Int J Antimicrob Agents.* 2019; 54(4): 496-501.
44. Buckner FS, Verlinde CL, La Flamme AC, Van Voorhis WC. Efficient technique for screening drugs for activity against *Trypanosoma cruzi* using parasites expressing beta-galactosidase. *Antimicrob Agents Chemother.* 1996; 40(11): 2592-7.
45. Annang F, Perez-Moreno G, Garcia-Hernandez R, Cordon-Obras C, Martin J, Tormo JR, et al. High-throughput screening platform for natural product-based drug discovery against 3 neglected tropical diseases: human African Trypanosomiasis, Leishmaniasis, and Chagas disease. *J Biomol Screen.* 2014; 20: 82-91.
46. Bettiol E, Samanovic M, Murkin AS, Raper J, Buckner F, Rodriguez A. Identification of three classes of heteroaromatic compounds with activity against intracellular *Trypanosoma cruzi* by chemical library screening. *PLoS Negl Trop Dis.* 2009; 3(2): e384.
47. Mandal S, Maharjan M, Ganguly S, Chatterjee M, Singh S, Buckner FS, et al. High-throughput screening of amastigotes of *Leishmania donovani* clinical isolates against drugs using a colorimetric beta-lactamase assay. *Indian J Exp Biol.* 2009; 47(6): 475-9.
48. Zhu X, Pandharkar T, Werbovetz K. Identification of new antileishmanial leads from hits obtained by high-throughput screening. *Antimicrob Agents Chemother.* 2012; 56(3): 1182-9.
49. Benítez D, Dibello E, Bonilla M, Comini MA. A simple, robust, and affordable bioluminescent assay for drug discovery against infective African trypanosomes. *Drug Dev Res [Internet].* 2020 [cited 2021 Dec 18]. Available from: <https://onlinelibrary.wiley.com/doi/10.1002/ddr.21634>.
50. Lang T, Goyard S, Lebastard M, Milon G. Bioluminescent *Leishmania* expressing luciferase for rapid and high throughput screening of drugs acting on amastigote-harboring macrophages and for quantitative real-time monitoring of parasitism features in living mice. *Cell Microbiol.* 2005; 7(3): 383-92.
51. Chandra N, Ramesh, Ashutosh, Goyal N, Suryawanshi SN, Gupta S. Antileishmanial agents part-IV: synthesis and antileishmanial activity of novel terpenyl pyrimidines. *Eur J Med Chem.* 2005; 40(6): 552-6.
52. Khraiweh M, Leed S, Roncal N, Johnson J, Sciotti R, Smith P, et al. Antileishmanial activity of compounds derived from the medicines for malaria venture open access box against intracellular *Leishmania major* amastigotes. *Am J Trop Med Hyg.* 2016; 94(2): 340-7.
53. De Rycker M, Hallyburton I, Thomas J, Campbell L, Wyllie S, Joshi D, et al. Comparison of a high-throughput high-content intracellular *Leishmania donovani* assay with an axenic amastigote assay. *Antimicrob Agents Chemother.* 2013; 57(7): 2913-22.
54. Alonso-Padilla J, Rodrı A. High throughput screening for anti - *Trypanosoma cruzi* drug discovery. *PLoS Negl Trop Dis.* 2014; 8(12): e3259.
55. Sharlow ER, Close D, Shun T, Leimgruber S, Reed R, Mustata G, et al. Identification of potent chemotypes targeting *Leishmania major* using a high-throughput, low-stringency, computationally enhanced, small molecule screen. *PLoS Negl Trop Dis.* 2009; 3(11): e540.
56. Shimony O, Jaffe CL. Rapid fluorescent assay for screening drugs on *Leishmania* amastigotes. *J Microbiol Methods.* 2008; 75: 196-200.
57. Eren RO, Kopelyanskiy D, Moreau D, Chapalay JB, Chambon M, Turcatti G, et al. Development of a semi-automated image-based high-throughput drug screening system. *Front Biosci.* 2018; 10: 242-53.
58. Gomes-Alves AG, Maia AF, Cruz T, Castro H, Tomás AM. Development of an automated image analysis protocol for quantification of intracellular forms of *Leishmania* spp. *PLoS One.* 2018; 13(8): e0201747.
59. Balaña-Fouce R, Pérez-Pertejo MY, Domínguez-Asenjo B, Gutiérrez-Corbo C, Reguera RM. Walking a tightrope: drug discovery in visceral leishmaniasis. *Drug Discov Today.* 2019; 24(5): 1209-16.
60. Peña I, Manzano MP, Cantizani J, Kessler A, Alonso-Padilla J, Bardera AI, et al. New compound sets identified from high throughput phenotypic screening against three kinetoplastid parasites: an open resource. *Sci Rep.* 2015; 5: 8771.
61. Caridha D, Vesely B, van Bocxlaer K, Arana B, Mowbray CE, Rafati S, et al. Route map for the discovery and pre-clinical development of new drugs and treatments for cutaneous leishmaniasis. *Int J Parasitol Drugs Drug Resist.* 2019; 11: 106-17.
62. Altamura F, Rajesh R, Catta-Preta CMC, Moretti NS, Cestari I. The current drug discovery landscape for trypanosomiasis and leishmaniasis: Challenges and strategies to identify drug targets. *Drug Dev Res [Internet].* 2020 [cited Dec 18]. Available from: <https://onlinelibrary.wiley.com/doi/10.1002/ddr.21664>.
63. Giuliano KA, DeBiasio RL, Dunlay RT, Gough A, Volosky JM, Zock J, et al. High-content screening: a new approach to easing key bottlenecks in the drug discovery process. *J Biomol Screen.* 1997; 2(4): 249-59.
64. Dorval T, Chanrion B, Cattin M-E, Stephan JP. Filling the drug discovery gap: is high-content screening the missing link? *Curr Opin Pharmacol.* 2018; 42: 40-5.
65. Buchser W, Collins M, Garyantes T, Guha R, Haney S, Lemmon V, et al. Assay development guidelines for image-based high content screening, high content analysis and high content imaging. In: Markossian S, Grossman A, Brimacombe K, Arkin M, Auld D, Austin CP, et al., editors. *Assay guidance manual.* Bethesda (MD): Eli Lilly & Company and the National Center for Advancing Translational Sciences; 2012.

66. Li S, Xia M. Review of high-content screening applications in toxicology. *Arch Toxicol.* 2019; 93(12): 3387-96.
67. Hefnawy A, Cantizani J, Peña I, Manzano P, Rijal S, Dujardin J-C, et al. Importance of secondary screening with clinical isolates for anti-leishmania drug discovery. *Sci Rep.* 2018; 8(1): 11765.
68. Siqueira-Neto JL, Song O-R, Oh H, Sohn J-H, Yang G, Nam J, et al. Antileishmanial high-throughput drug screening reveals drug candidates with new scaffolds. *PLoS Negl Trop Dis.* 2010; 4(5): e675.
69. Alonso-Padilla J, Cotillo I, Presa JL, Cantizani J, Peña I, Bardera AI, et al. Automated high-content assay for compounds selectively toxic to *Trypanosoma cruzi* in a myoblastic cell line. *PLoS Negl Trop Dis.* 2015; 9: e0003493.
70. Moraes CB, Giardini MA, Kim H, Franco CH, Araujo-Junior AM, Schenkman S, et al. Nitroheterocyclic compounds are more efficacious than CYP51 inhibitors against *Trypanosoma cruzi*: implications for Chagas disease drug discovery and development. *Sci Rep.* 2014; 4: 4703.
71. Portella DCN, Rossi EA, Paredes BD, Bastos TM, Meira CS, Nonaka CVK, et al. A novel high-content screening-based method for anti-*Trypanosoma cruzi* drug discovery using human-induced pluripotent stem cell-derived cardiomyocytes. *Stem Cells Int.* 2021; 2021: 2642807.
72. Sykes ML, Avery VM. 3-pyridyl inhibitors with novel activity against *Trypanosoma cruzi* reveal *in vitro* profiles can aid prediction of putative cytochrome P450 inhibition. *Sci Rep.* 2018; 8(1): 4901.
73. MacLean LM, Thomas J, Lewis MD, Cotillo I, Gray DW, De Rycker M. Development of *Trypanosoma cruzi in vitro* assays to identify compounds suitable for progression in Chagas' disease drug discovery. *PLoS Negl Trop Dis.* 2018; 12(7): e0006612.
74. Tegazzini D, Díaz R, Aguilar F, Peña I, Presa JL, Yardley V, et al. A replicative *in vitro* assay for drug discovery against *Leishmania donovani*. *Antimicrob Agents Chemother.* 2016; 60(6): 3524-32.
75. Lamotte S, Aulner N, Späth GF, Prina E. Discovery of novel hit compounds with broad activity against visceral and cutaneous *Leishmania* species by comparative phenotypic screening. *Sci Rep.* 2019; 9(1): 438.
76. Aulner N, Danckaert A, Rouault-Hardoin E, Desrivot J, Helynck O, Commere P-H, et al. High content analysis of primary macrophages hosting proliferating *Leishmania* amastigotes: application to anti-leishmanial drug discovery. *PLoS Negl Trop Dis.* 2013; 7(4): e2154.
77. Fehling H, Niss H, Bea A, Kottmayr N, Brinker C, Hoenow S, et al. High content analysis of macrophage-targeting EhP1b-compounds against cutaneous and visceral *Leishmania* species. *Microorganisms.* 2021; 9(2): 422.
78. Dagley MJ, Saunders EC, Simpson KJ, McConville MJ. High-content assay for measuring intracellular growth of *Leishmania* in human macrophages. *Assay Drug Dev Technol.* 2015; 13(7): 389-401.
79. Sykes ML, Avery VM. Development and application of a sensitive, phenotypic, high-throughput image-based assay to identify compound activity against *Trypanosoma cruzi* amastigotes. *Int J Parasitol Drugs Drug Resist.* 2015; 5(3): 215-28.
80. Miskinyte M, Dawson JC, Makda A, Doughty-Shenton D, Carragher NO, Schnauffer A. A novel high-content phenotypic screen to identify inhibitors of mitochondrial DNA maintenance in trypanosomes. *Antimicrob Agents Chemother* [Internet]. 2021 [cited 2021 Dec 18]. Available from: <https://journals.asm.org/doi/10.1128/AAC.01980-21>.
81. Melo-Filho CC, Braga RC, Muratov EN, Franco CH, Moraes CB, Freitas-Junior LH, et al. Discovery of new potent hits against intracellular *Trypanosoma cruzi* by QSAR-based virtual screening. *Eur J Med Chem.* 2019; 163: 649-59.
82. Siqueira-Neto JL, Moon S, Jang J, Yang G, Lee C, Moon HK, et al. An image-based high-content screening assay for compounds targeting intracellular *Leishmania donovani* amastigotes in human macrophages. *PLoS Negl Trop Dis.* 2012; 6(6): e1671.
83. Alcântara LM, Ferreira TCS, Fontana V, Chatelain E, Moraes CB, Freitas-Junior LH. A multi-species phenotypic screening assay for leishmaniasis drug discovery shows that active compounds display a high degree of species-specificity. *Molecules.* 2020; 25(11): 2551.
84. Roquero I, Cantizani J, Cotillo I, Manzano MP, Kessler A, Martín JJ, et al. Novel chemical starting points for drug discovery in leishmaniasis and Chagas disease. *Int J Parasitol Drugs Drug Resist.* 2019; 10: 58-68.
85. Bernatchez JA, Chen E, Hull MV, McNamara CW, McKerrow JH, Siqueira-Neto JL. High-throughput screening of the ReFRAME library identifies potential drug repurposing candidates for *Trypanosoma cruzi*. *Microorganisms.* 2020; 8(4): 472.
86. Boudreau PD, Miller BW, McCall L-I, Almaliti J, Reher R, Hirata K, et al. Design of Gallinamide A analogs as potent inhibitors of the cysteine proteases human Cathepsin L and *Trypanosoma cruzi* Cruzain. *J Med Chem.* 2019; 62(20): 9026-44.
87. Ekins S, de Siqueira-Neto JL, McCall L-I, Sarker M, Yadav M, Ponder EL, et al. Machine learning models and pathway genome data base for *Trypanosoma cruzi* drug discovery. *PLoS Negl Trop Dis.* 2015; 9(6): e0003878.
88. Neitz RJ, Chen S, Supek F, Yeh V, Kellar D, Gut J, et al. Lead identification to clinical candidate selection: drugs for Chagas disease. *J Biomol Screen.* 2014; 20: 101-11.
89. Engel JC, Ang KKH, Chen S, Michelle R, Mckerrow JH, Doyle PS, et al. Image-based high-throughput drug screening targeting the intracellular stage of *Trypanosoma cruzi*, the agent of Chagas' disease. *Antimicrob Agents Chemother.* 2010; 54(8): 3326-34.
90. Genovesio A, Giardini MA, Kwon YJ, Dossin FM, Choi SY, Kim NY, et al. Visual genome-wide RNAi screening to identify human host factors required for *Trypanosoma cruzi* infection. *PLoS One.* 2011; 6(5): e19733.
91. Liu D, Uzonna JE. The early interaction of *Leishmania* with macrophages and dendritic cells and its influence on the host immune response. *Front Cell Infect Microbiol.* 2012; 2: 83.
92. Hendrickx S, Van Bockstal L, Caljon G, Maes L. In-depth comparison of cell-based methodological approaches to determine drug susceptibility of visceral *Leishmania* isolates. *PLoS Negl Trop Dis.* 2019; 13(12): e0007885.
93. Bosc D, Mouray E, Cojean S, Franco CH, Loiseau PM, Freitas-Junior LH, et al. Highly improved antiparasitic activity after introduction of an N-benzylimidazole moiety on protein farnesyltransferase inhibitors. *Eur J Med Chem.* 2016; 109: 173-86.
94. De Rycker M, Thomas J, Riley J, Brough SJ, Miles TJ, Gray DW. Identification of trypanocidal activity for known clinical compounds using a new *Trypanosoma cruzi* hit-discovery screening cascade. *PLoS Negl Trop Dis.* 2016; 10(4): e0004584.
95. Phan T-N, Baek K-H, Lee N, Byun SY, Shum D, No JH. *In vitro* and *in vivo* activity of mTOR kinase and PI3K inhibitors against *Leishmania donovani* and *Trypanosoma brucei*. *Molecules.* 2020; 25(8): 1980.
96. De Muylder G, Ang KKH, Chen S, Arkin MR, Engel JC, McKerrow JH. A screen against *Leishmania* intracellular amastigotes: comparison to a promastigote screen and identification of a host cell-specific hit. *PLoS Negl Trop Dis.* 2011; 5(7): e1253.
97. Fesser AF, Braissant O, Olmo F, Kelly JM, Mäser P, Kaiser M. Non-invasive monitoring of drug action: a new live *in vitro* assay design for Chagas' disease drug discovery. *PLoS Negl Trop Dis.* 2020; 14(7): e0008487.

98. Zulfiqar B, Jones AJ, Sykes ML, Shelper TB, Davis RA, Avery VM. Screening a natural product-based library against kinetoplastid parasites. *Molecules*. 2017; 22(10): 1715.
99. Duffy S, Sykes ML, Jones AJ, Shelper TB, Simpson M, Lang R, et al. Screening the medicines for malaria venture pathogen box across multiple pathogens reclassifies starting points for open-source drug discovery. *Antimicrob Agents Chemother*. 2017; 61(9): e00379-17.
100. Moon S, Siqueira-Neto JL, Moraes CB, Yang G, Kang M, Freitas-Junior LH, et al. An image-based algorithm for precise and accurate high throughput assessment of drug activity against the human parasite *Trypanosoma cruzi*. *PLoS One*. 2014; 9(2): e87188.
101. Dean S, Gould MK, Dewar CE, Schnauffer AC. Single point mutations in ATP synthase compensate for mitochondrial genome loss in trypanosomes. *Proc Natl Acad Sci USA*. 2013; 110(36): 14741-6.
102. Lewis MD, Fortes FA, Taylor MC, Burrell-Saward H, McLatchie AP, Miles MA, et al. Bioluminescence imaging of chronic *Trypanosoma cruzi* infections reveals tissue-specific parasite dynamics and heart disease in the absence of locally persistent infection. *Cell Microbiol*. 2014; 16(9): 1285-300.
103. Ferreira BL, Orikaza CM, Cordero EM, Mortara RA. *Trypanosoma cruzi*: single cell live imaging inside infected tissues. *Cell Microbiol*. 2016; 18(6): 779-83.
104. Portapilla GB, Pereira LM, da Costa CMB, Providello MV, Oliveira PAS, Goulart A, et al. Phenothiazinium dyes are active against *Trypanosoma cruzi* *in vitro*. *Biomed Res Int*. 2019; 2019: 8301569.
105. Lecoeur H, de La Llave E, Osorio Y Fortéa J, Goyard S, Kiefer-Biasizzo H, Balazuc A-M, et al. Sorting of *Leishmania*-bearing dendritic cells reveals subtle parasite-induced modulation of host-cell gene expression. *Microbes Infect*. 2010; 12(1): 46-54.
106. Katsuno K, Burrows JN, Duncan K, van Huijsduijnen RH, Kaneko T, Kita K, et al. Hit and lead criteria in drug discovery for infectious diseases of the developing world. *Nat Rev Drug Discov*. 2015; 14(11): 751-8.
107. Yang G, Lee N, Ioset J-R, No JH. Evaluation of parameters impacting drug susceptibility in intracellular *Trypanosoma cruzi* assay protocols. *SLAS Discov*. 2017; 22(2): 125-34.
108. Dantas RF, Evangelista TCS, Neves BJ, Senger MR, Andrade CH, Ferreira SB, et al. Dealing with frequent hitters in drug discovery: a multidisciplinary view on the issue of filtering compounds on biological screenings. *Expert Opin Drug Discov*. 2019; 14(12): 1269-82.
109. Senger MR, Fraga CAM, Dantas RF, Silva Jr FP. Filtering promiscuous compounds in early drug discovery: is it a good idea? *Drug Discov Today*. 2016; 21(6): 868-72.
110. Costa FC, Francisco AF, Jayawardhana S, Calderano SG, Lewis MD, Olmo F, et al. Expanding the toolbox for *Trypanosoma cruzi*: a parasite line incorporating a bioluminescence-fluorescence dual reporter and streamlined CRISPR/Cas9 functionality for rapid *in vivo* localisation and phenotyping. *PLoS Negl Trop Dis*. 2018; 12(4): e0006388.
111. Calvo-Alvarez E, Cren-Travaillé C, Cruzols A, Rotureau B. A new chimeric triple reporter fusion protein as a tool for *in vitro* and *in vivo* multimodal imaging to monitor the development of African trypanosomes and *Leishmania* parasites. *Infect Genet Evol*. 2018; 63: 391-403.